One-Pot *In Situ* Ball Milling Preparation of Polymer/Graphene Nanocomposites

Hang Wu, Weifeng Zhao, Guohua Chen

Department of Polymer Science and Engineering, Huaqiao University, Xiamen 361021, China

Received 5 April 2011; accepted 2 August 2011
DOI 10.1002/app.35413
Published online in Wiley Online Library (wileyonlinelibrary.com).

ABSTRACT: A one-pot method which involves peeling graphite nanosheets (GNs) off into graphenes in polymer solution and *in situ* forming polymer/graphene sheets nanocomposites by using ball milling is presented. Via this approach, nanocomposites based on maleic anhydride grafted poly (ethylene-*co*-vinyl acetate) (EVA-*g*-MAH) and graphene sheets comprising one to five layers were accomplished. The resulted EVA-*g*-MAH/graphene nanocomposites displayed a percolation threshold around 5.0 wt %, much lower than that of the EVA-*g*-MAH/GNs nanocomposites prepared by direct solution blending ($\sim$ 13.0 wt %). The nanocomposite containing 10 wt % of graphene sheets exhibited a higher maximum decomposition temperature by $\sim$ 10°C when compared with the virgin polymer and the corresponding nanocomposite loaded with 10 wt % of GNs. © 2012 Wiley Periodicals, Inc. J Appl Polym Sci 000: 000–000, 2012

Key words: exfoliated graphite; graphite nanosheets; graphene; polymer composites; ball milling

INTRODUCTION

During the past years, intense research on polymer/graphite nanocomposites has been promoted to develop polymer materials for applications where good electrical and mechanical properties are often required.[1–11] The critical issue for the polymer/graphite nanocomposite fabrication is to ensure a good exfoliation and dispersion of graphite in polymer matrices. The exfoliation of graphite fillers allows them to provide the maximum efficiency for a given volume percentage. Compared with the conventional micrometer-size graphite particles, exfoliated graphite nanoplatelets such as expanded graphite (EG) and graphite nanosheets (GNs) produced by chemical routes via graphite intercalation compounds (GIC) have been proved much more efficient in reinforcement. For example, with the benefit of high aspect ratio, the EG and GNs fillers tend to more easily form conducting networks in polymers leading to electrically conductive composites with a low percolation threshold.[12–15] However, the graphite nanoplatelets such as GNs are still composed of hundreds of single carbon layers held together by van der Waals-like forces. To yield higher reinforcement efficiency, they are expected to be further exfoliated toward atom-thick graphenes as sufficiently as possible and dispersed throughout polymer matrix properly.

Besides minimized thickness, the graphene sheets also possess various fascinating properties such as high values of Young's modulus and fracture strength,[16] remarkable thermal conductivity,[17] extraordinary mobility of charge carriers,[18] superior specific surface area,[19] and novel relativistic quantum electric transport behaviors,[20] which make them an attractive candidate to modify polymers. In recent years, significant success has been achieved for polymer nanocomposites with graphene sheets derived from graphite oxide (GO). It has been demonstrated that when the graphene oxide sheets are finely dispersed and reduced in polymer matrix, the properties of the final graphene composite tend to rival those for corresponding polymer composite reinforced with single-walled carbon nanotubes.[21] Nevertheless, how to modify polymers with unoxidized pristine graphene sheets remains an important open question in polymer nanocomposites.

As has been demonstrated by our previous report, single- and few-layer graphene sheets ($\leq$3 layers) were obtained from the starting graphite nanoplatelets using the wet ball milling method.[22,23] Here, we attempt to employ wet ball milling to exfoliate multilayered GNs toward graphene sheets in the medium of maleic anhydride grafted poly(ethylene-*co*-vinyl acetate) (EVA-*g*-MAH) toluene solution to produce EVA-*g*-MAH/graphene sheets nanocomposites *in situ*. The main advantage of this technique is twofold: (1) the wet ball milling method is certainly

Correspondence to: G. Chen (hdcgh@hqu.edu.cn).
Contract grant sponsor: Natural Science Foundation of Fujian Province; contract grant number: E0820001.
Contract grant sponsor: Science Foundation of Xiamen; contract grant number: 3502Z20103032.

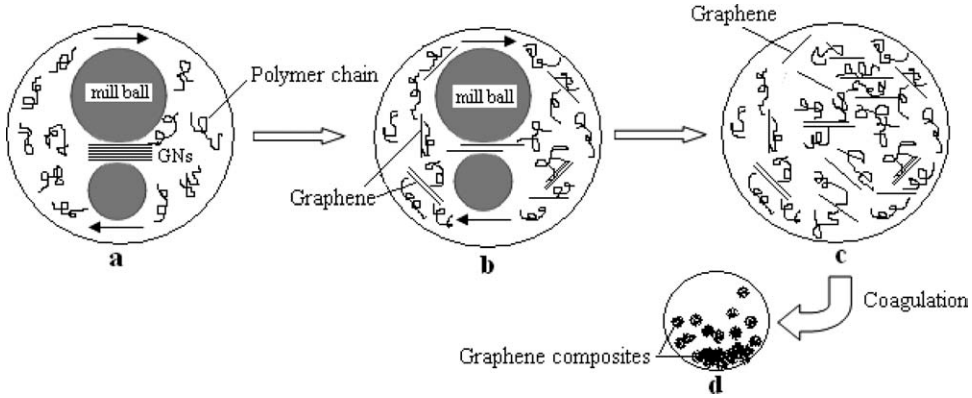

Figure 1 Schematic illustration for the *in situ* creation of polymer/graphene nanocomposites by using ball milling: (a) GNs dispersed in polymer solution are exfoliated by rotating balls; (b) graphene sheets are formed *in situ* in polymer solution via ball milling; (c) graphenes are individually dispersed in polymer solution; (d) after coagulation, graphene nanocomposites are created.

superior to the traditional mixing strategy of mechanical stirring in terms of filler dispersion; and (2) the presence of host polymer in medium solution during the graphite exfoliation step is effective to modifying the resulted graphene layers *in situ* to improve the homogeneity of the graphene sheets in final composites.

EXPERIMENTAL

Fabrication of composites

GNs fillers were prepared by using sonication to break EG apart in ethanol solution as reported.[24] The different mass fractions of dried GNs were dispersed into toluene (Xilong Chemical Reagent Co. Ltd, China) via a short time sonication about 2 min, and subsequently added into the toluene solutions containing 20 wt % EVA-*g*-MAH resin (Density: 0.95 g/cm^3; melt index at 2.16 kg/190°C: 1–15 g/10 min; melt point: ~ 71°C; grafting ratio: 1.1%; VA content: 28%; Sinopharm Chemical Reagent Co. Ltd, China) drop by drop with thoroughly stirring. After being sonicated for another 20 min, the GNs suspension in EVA-*g*-MAH toluene solution was subjected to continuous ball mill for 30 h in a planetary with a low rotational speed of 300 rpm at room temperature [Fig. 1(a)]. Due to the weak van der Waals-like coupling between graphite layers, the GNs were readily peeled off toward graphenes *in situ* under the shear forces applied by the rotating balls [Fig. 1(b)]. A dark homogeneous mixture system containing individually dispersed graphene sheets was then obtained [Fig. 1(c)]. By adding excessive ethanol to the solution, the coagulation of the polymer composites was accomplished [Fig. 1(d)]. The coagulated graphene nanocomposites were isolated via subsequent centrifugation; kept for vacuum drying at 50°C till there was no practically weight variation. The as-prepared composite samples for electrical conductivity test were pressed between brass plates into a thin film, with a thickness of around 0.2–0.25 mm, using 0.2 mm-thick spacers in a hydraulic hot press at 180° under the pressure of 2 MPa. For comparison, the composites filled with GNs were also prepared using a conventional sonication blending method.[25] Typically, different mass fractions of GNs were dispersed in toluene with the assistance of sonication at room temperature, which were then mixed with toluene solutions containing 20 wt % EVA-*g*-MAH, and sonicated for 10 h at room temperature. The composites with different filler concentrations in the range of 1–20 wt % were prepared.

Characterization and property measurement

Hot-pressed composite samples having ~ 2.0 mm thickness were cut into circular pieces with a diameter of 20 mm. X-ray diffraction(XRD) was conducted on an X-ray diffractometer of D8-Advance (Germany) to scan the sample surface from 5° to 32° of 2θ at a rate of 2° per minute. Transmission electron microscopy (TEM) image was acquired on microtomed composite slices using a JEM-2010 JEOL transmission electron microscope. Volume resistivity ρ of the composites was measured by using a DT 9205A multimeter ($\rho < 10^8$ Ωcm) and ZC-36 high resistance tester ($\rho > 10^8$ Ωcm). Thermo gravimetric analysis (TGA) was carried out on a Perkin-Elmer TGA instrument TA-5200 at a heating rate 10°C/min in nitrogen atmosphere. Differential thermo gravimetric analysis (DTG) was represented in terms of the first derivative plots of the TGA curves.

RESULTS AND DISCUSSION

TEM analysis

To achieve good exfoliation of GNs toward graphene sheets in EVA-*g*-MAH solution is the most critical

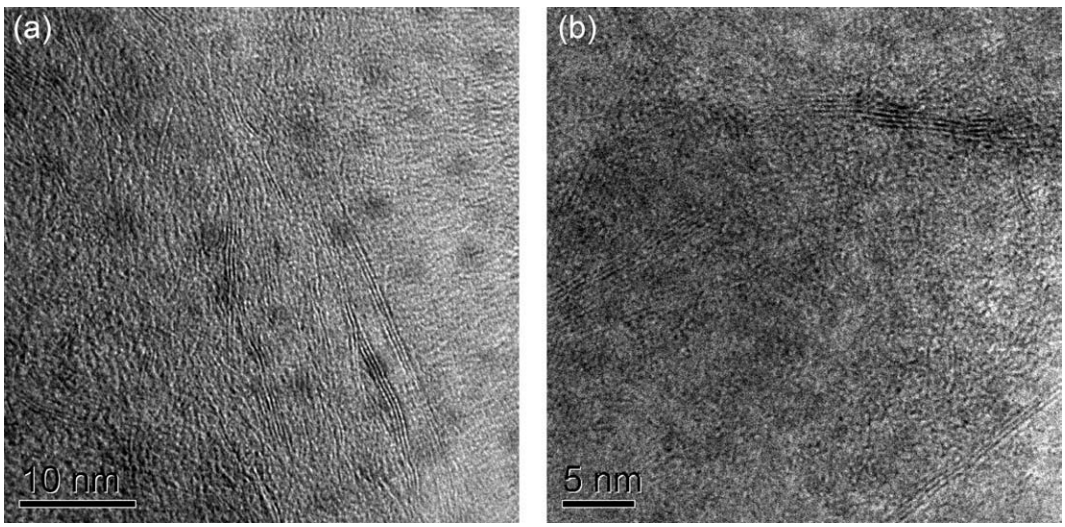

Figure 2 High-resolution TEM image of microtomed polymer/graphene nanocomposite.

issue for the successful development of graphene nanocomposites. This had been well accomplished via the ball milling route. As shown in Figure 2, the dark lines corresponding to the cross sections of the embedded single and few-layer graphene sheets comprising one to five layers can be readily identified from the high-resolution TEM image of the microtomed composite slice, suggesting a successful achievement of EVA-*g*-MAH/graphene nanocomposites.

X-ray diffraction

The exfoliation of GNs inside the EVA-*g*-MAH matrix was also convinced by the XRD pattern of the composite. As shown in Figure 3, in contrast to the XRD pattern of the EVA-*g*-MAH/GNs composite which displays a sharp diffraction peak at $2\theta = 26.4^\circ$ due to the scanning from 002 plane of GNs, the EVA-*g*-MAH composite with graphene sheets shows a diffraction pattern almost without any 002 peak of graphite. This indicates that the multilayered graphitic structure of GNs was lost significantly and the GNs were well delaminated into graphenes in the final composite after being exfoliated by ball milling.

Electrical properties

Figure 4 shows the logarithmic volume resistivity of the EVA-*g*-MAH composites as a function of filler weight fraction for the EVA-*g*-MAH/GNs and EVA-*g*-MAH/graphenes nanocomposites, respectively. The addition of conducting graphite nanofillers significantly lowered the resistivity of EVA-*g*-MAH composites. The S-shaped curves indicate that both the nanocompsites with either GNs or graphenes exhibit typical percolation transition from an insulator to semiconductor. As expected, the percolation threshold value of the EVA-*g*-MAH/graphenes nanocomposites (estimated to be about 5.0 wt % from the percolation curve) is markedly lower than that of the EVA-*g*-MAH/GNs composites prepared by direct sonication–assisted blending, which is $\sim$ 13.0 wt %. The low percolation threshold for the EVA-*g*-MAH/graphenes nanocomposites is attributed to the much higher aspect ratio of graphene sheets compared with that of GNs, as well as the homogeneous graphene dispersion in the polymer matrix. This gives further evidence of the exfoliation of GNs toward graphenes in EVA-*g*-MAH matrix.

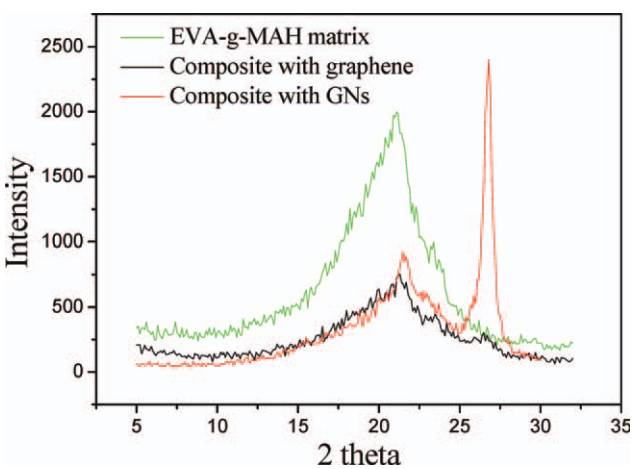

Figure 3 XRD patterns of pure EVA-*g*-MAH and its composites containing 10 wt % of GNs and graphenes. [Color figure can be viewed in the online issue, which is available at wileyonlinelibrary.com.]

Thermal stability

Figure 5 demonstrates the TGA and DTG plots of the neat EVA-*g*-MAH and its nanocomposites reinforced by graphene sheets and GNs, respectively. All the samples display a two-stage degradation curve due to the decomposition of side and main chains of EVA-*g*-MAH [Fig. 5(a)]. However, their thermal stabilities are some clearly different compared with each other. As observed from the DTG plots in Figure 5(b) and reported in Table I, compared with the DTG peaks of pure EVA-*g*-MAH, the addition of GNs almost had no effects on the matrix decomposition temperature which is $\sim$ 497°C, but only decreased the degradation rate, especially in the second degradation phase. However, the maximum decomposition temperature was improved notably to $\sim$ 508°C for the graphene-reinforced composites where the GNs had been exfoliated by ball milling processing, due to the more effective heat shielding[26] derived from graphene sheets in comparison to that from the multilayered GNs.

CONCLUSIONS

A one-pot *in situ* method for manufacturing polymer/graphene sheets nanocomposites was proposed via exfoliating GNs in EVA-*g*-MAH solution using wet ball milling process. The exfoliation of GNs into graphene sheets improved the comprehensive performance to polymer matrix greatly. Single- and few-layer graphene sheets have been successfully achieved by using the wet ball milling method from GNs in polymer solution. As a result, a much lower percolation threshold and higher thermal stability were achieved in the final graphene nanocomposites compared with those of the traditional nanocomposites reinforced with GNs. However, the yield of the monolayer graphene is related to many parameters such as diameters of milling balls, period of milling times, the content of GNs in the toluene medium, the speed of centrifugation, and so on. The study of optimal conditions for the ball milling exfoliation is currently under way.

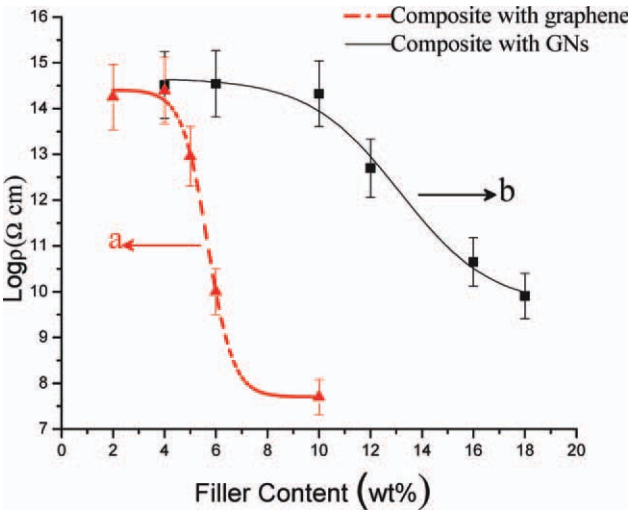

Figure 4 Curves of resistivity ρ versus filler content for composites with graphenes (a) and GNs (b). [Color figure can be viewed in the online issue, which is available at wileyonlinelibrary.com.]

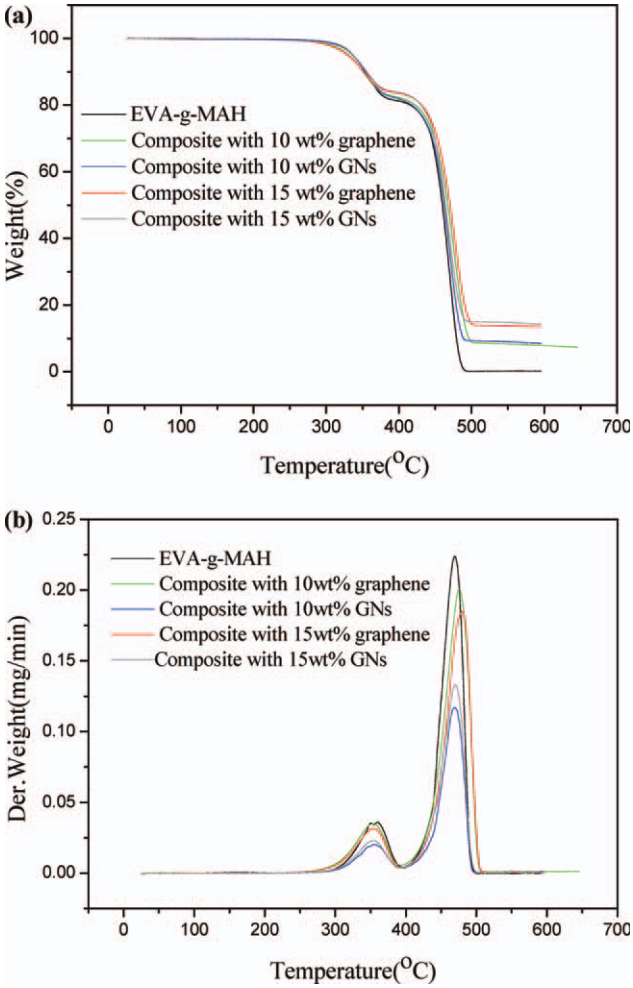

Figure 5 TGA (a) and DTG (b) curves of EVA-*g*-MAH and its composites with GNs and graphene sheets. [Color figure can be viewed in the online issue, which is available at wileyonlinelibrary.com.]

TABLE I
Temperature of Maximum Degradation and Maximum Rate of Degradation for Grafted Polymer and Composites

Samples	Temperature of maximum degradation (°C)	Maximum rate of degradation (mg/min)
EVA-*g*-MAH	497	0.22
Composite with 10 wt % graphene	506	0.20
Composite with 15 wt % graphene	508	0.18
Composite with 10 wt % GNs	496	0.13
Composite with 15 wt % GNs	497	0.11

References

1. Zheng, W. G.; Wong, S. C. Compos Sci Technol 2003, 63, 225.
2. Wang, W. P.; Pan, C. Y.; Wu, J. S. J Phys Chem Solids 2005, 66, 1695.
3. Xiao, P.; Xiao, M.; Gong, K. Polymer 2001, 42, 4813.
4. Chen, D. Q.; Yang, J. Y.; Chen, G. H. Compos A 2010, 41, 1636.
5. Zheng, W. G.; Wong, S. C.; Sue, H. J. Polymer 2002, 43, 6767.
6. Wei, L.; Lin, H. F.; Chen, G. H. Polymer 2006, 47, 4440.
7. Du, X. S.; Xiao, M.; Meng, Y. Z.; Hay, A. S. Polymer 2004, 45, 6713.
8. Wakabayashi, K.; Pierre, C.; Dikin, D. A.; Ruoff, R. S; Ramanathan, T.; Brinson, L. C.; Torkelson, J. M. Macromolecules 2008, 41, 1905.
9. Pramoda, K. P.; Linh, N. T. T.; Tang, P. S.; Tjiu, W. C.; Goh, S. H.; He, C. B. Compos Sci Technol 2010, 70, 578.
10. Yang, J.; Tian, M.; Jia, Q. X.; Shi, J. H.; Zhang, L. Q.; Lim, S. H.; Yu, Z. Z.; Mai, Y. W. Acta Mater 2007, 55, 6372.
11. Wang, L. W.; Chen, G. H. J Appl Polym Sci 2010, 116, 2029.
12. Chen, G. H.; Lu, J. R.; Lu, W.; Wu, D. J.; Wu, C. L. Polym Int 2005, 54, 1689.
13. Chen, L.; Chen, G. H.; Lu, L. Adv Funct Mater 2007, 17, 898.
14. Song, L. N.; Xiao, M.; Meng, Y. Z. Compos Sci Technol 2006, 66, 2156.
15. Chen, G. H.; Wu, C. L.; Weng, W. G.; Wu, D. J.; Yan, W. L. Polymer 2003, 44, 1781.
16. Lee, C.; Wei, X.; Kysar, J. W.; Hone, J. Science 2008, 321, 385.
17. Balandin, A. A.; Ghosh, S.; Bao, W. Z.; Calizo, I. Teweldebrhan, D.; Miao, F.; Lau, C. N. Nano Lett 2008, 8, 902.
18. Bolotin, K. I.; Sikes, K. J.; Jiang, Z.; Klima, M.; Fudenberg, G.; Hone, J. Hone, J.; Kim, P.; Stormer, H. L. Solid State Commun 2008, 146, 351.
19. Stoller, M. D.; Park, S.; Zhu, Y.; An, J.; Ruoff, R. S. Nano Lett 2008, 8, 3498.
20. Zhang, Y.; Tan, Y. W.; Stormer, H. L.; Kim, P. Nature 2005, 438, 201.
21. Stankovich, S.; Dikin, D. A.; Dommett, G. H. B.; Kohlhaas, K. M.; Zimney, E. J.; Stach, E. A.; Piner, R. D.; Nguyen, S. B. T.; Ruoff, R. S. Nature 2006, 442, 282.
22. Zhao, W. F.; Fang, M.; Wu, F. R.; Wu, H.; Wang, L. W.; Chen, G. H. J Mater Chem 2010, 20, 5817.
23. Wu, H.; Zhao, W. F.; Hu, H. W.; Chen, G. H. J Mater Chem 2011, 21, 8626.
24. Chen, G. H.; Wu, D. J.; Weng, W. G.; Wu, C. L. Carbon 2003, 41, 619.
25. Chen, G. H.; Weng, W.G.; Wu, D. J.; Wu, C. L. Eur Polym J 2003, 39, 2329.
26. Weng, W. G.; Chen, G. H.; Wu, D. J.; Chen, X. F.; Lu, J. R.; Wang, P. P. J Polym Sci Part B: Polym Phys 2004, 42, 2844.